Adhesion Force Studies of Janus Nanoparticles

Li-Ping Xu, Sulolit Pradhan, and Shaowei Chen*

*Department of Chemistry and Biochemistry, University of California, 1156 High Street,
Santa Cruz, California 95064*

Janus nanoparticles represent a unique nanoscale analogue to the conventional surfactant molecules, exhibiting hydrophobic characters on one side and hydrophilic characters on the other. Yet, direct visualization of the asymmetric surface structures of the particles remains a challenge. In this paper, we used a simple technique based on AFM adhesion force measurements to examine the two distinctly different hemispheres of the Janus particles at the molecular level. Experimentally, the Janus nanoparticles were prepared by ligand exchange reactions at the air−water interface. The particles were then immobilized onto a substrate surface with the particle orientation controlled by the chemical functionalization of the substrate surface, and an AFM adhesion force was employed to measure the interactions between the tip of a bare silicon probe and the Janus nanoparticles. It was found that when the hydrophilic side of the particles was exposed, the adhesion force was substantially greater than that with the hydrophobic side exposed, as the silicon probes typically exhibit hydrophilic properties. These studies provide further confirmation of the amphiphilic nature of the Janus nanoparticles.

Introduction

Nanoparticles have long been fascinating objects due to their potential applications as novel building blocks for the fabrication of next-generation optical/electronic devices.[1−6] Thus, a typical objective in colloid and nanoparticle science is to obtain particles with a homogeneous chemical composition, which will have value in applications such as painting, ceramics, and photonics.[7] Recently, the preparation of asymmetrically functionalized particles whose surface chemical composition differs on two sides of the particle (Janus as suggested by de Gennes)[8] has received much attention.[9−11] They may be used as unique structural elements for supraparticular assemblies[12,13] that would not be accessible with homogeneously functionalized counterparts.[14] In addition, they can self-organize and select left from right or top from bottom to yield supraparticular architectures in a pre-programmed fashion, akin to proteins. Beyond their use as elementary building blocks for organized assemblies, Janus particles are also promising with respect to numerous other applications. For instance, Janus particles with oppositely charged hemispheres have a large dipole moment that may allow remote positioning in an electric field.[15−18] If the Janus particles have both electrical and color anisotropy, they may be used in electronic paper.[19,20] Janus particles coated with different chemical groups can also be derivatized into bifunctional carriers useful for catalysis, sensing, drug delivery, etc. Janus particles with an electron donor side and an acceptor side may be exploited as nanoscale machinery in the conversion of solar energy into electrical currents. The amphiphilic Janus particles with hydrophilic and hydrophobic hemispheres also can be used as particular surfactants in the stabilization of water-in-oil or oil-in-water emulsions.[21,22]

Yet, as pointed out by Duguet et al.,[22] the direct visualization of the surface dis-symmetry of these nanoparticles is not a simple task, as the difference between the two hemispheres is at the molecular level. Atomic force microscopy (AFM), which was originally used to obtain surface topography of materials, is a rapidly developing technique with high spatial resolution, high sensitivity, minimum sample consumption, low experimental variations, and no environmental limitation. It also offers a convenient way to precisely measure the interactions between its probe tip and the substrate surface. AFM force−distance measurements have become a fundamental tool in the fields of surface science, biochemistry, and material science. In the past few years, there have been numerous reports on probing different chemical and biochemical interactions by using AFM-based techniques.[23−25]

In this study, we employ AFM-based adhesion force measurements to characterize the amphiphilic nature of Janus nanoparticles. These nanosized particles[26] were prepared by ligand exchange reactions of a Langmuir monolayer of hydrophobic

* Corresponding author. E-mail: schen@chemistry.ucsc.edu.

(1) Zhang, Z. L.; Glotzer, S. C. *Nano Lett.* **2004,** *4,* 1407−1413.
(2) Schmid, G. *Clusters and Colloids: From Theory to Applications*; VCH: Weinheim, Germany, 1994.
(3) Turton, R. *The Quantum Dot: A Journey into the Future of Microelectronics*; Oxford University Press: New York, 1995.
(4) Craighead, H. G. *Science* **2000,** *290,* 1532−1535.
(5) Quake, S. R.; Scherer, A. *Science* **2000,** *290,* 1536−1540.
(6) Jager, E. W. H.; Smela, E.; Inganas, O. *Science* **2000,** *290,* 1540−1545.
(7) Qi, M. H.; Lidorikis, E.; Rakich, P. T.; Johnson, S. G.; Joannopoulos, J. D.; Ippen, E. P.; Smith, H. I. *Nature* **2004,** *429,* 538−542.
(8) de Gennes, P. G. *Science* **1992,** *256,* 495−497.
(9) Hong, L.; Jiang, S.; Granick, S. *Langmuir* **2006,** *22,* 9495−9499.
(10) Binks, B. P.; Fletcher, P. D. I. *Langmuir* **2001,** *17,* 4708−4710.
(11) Nisisako, T.; Torii, T.; Takahashi, T.; Takizawa, Y. *Adv. Mater.* **2006,** *18,* 1152−1156.
(12) Li, Z.; Lee, D.; Rubner, M. F.; Cohen, R. E. *Macromolecules* **2005,** *38,* 7876−7879.
(13) Nie, Z.; Li, W.; Seo, M.; Xu, S.; Kumacheva, E. *J. Am. Chem. Soc.* **2006,** *128,* 9408−9412.
(14) Glotzer, S. C. *Science* **2004,** *306,* 419−420.
(15) Takei, H.; Shimizu, N. *Langmuir* **1997,** *13,* 1865−1868.
(16) Cayre, O.; Paunov, V. N.; Velev, O. D. *Chem. Commun.* **2003,** 2296−2297.

(17) Cayre, O.; Paunov, V. N.; Velev, O. D. *J. Mater. Chem.* **2003,** *13,* 2445−2450.
(18) Paunov, V. N.; Cayre, O. J. *Adv. Mater.* **2004,** *16,* 788−791.
(19) Millman, B. K., Jr.; Prevo, B. G; Velev, O. D. *Nat. Mater.* **2005,** *4,* 98−102.
(20) Fialkowski, M. B. A.; Grzybowski, B. A. *Nat. Mater.* **2005,** *4,* 93−97.
(21) Binks, B. P.; Lumsdon, S. O. *Langmuir* **2001,** *17,* 4540−4547.
(22) Perro, A.; Reculusa, S.; Ravaine, S.; Bourgeat-Lami, E. B.; Duguet, E. *J. Mater. Chem.* **2005,** *15,* 3745−3760.
(23) Jiang, Y. X.; Zhu, C. F.; Ling, L. S.; Wan, L. J.; Fang, X. H.; Bai, C. *Anal. Chem.* **2003,** *75,* 2112−2116.
(24) Moy, V. T.; Florin, E. L.; Gaub, H. E. *Science* **1994,** *266,* 257−259.
(25) Kado, S.; Yamada, K.; Kimura, K. *Langmuir* **2004,** *20,* 3259−3263.
(26) Pradhan, S.; Xu, L.; Chen, S. *Adv. Funct. Mater.* **2007,** in press.

alkanethiolate-passivated gold nanoparticles at relatively high surface pressures with hydrophilic thiol derivatives injected into the water subphase. In our previous studies,[26] the amphiphilic characters of these particles were examined by various spectroscopic techniques, including contact angle, dynamic light scattering, FTIR, NMR, and UV−vis measurements. It was found that approximately 50% of the protecting monolayer of the Janus particles consisted of the original hydrophobic hexanethiolate ligands, whereas the other 50% was the hydrophilic 3-mercaptopropane-1,2-diol (MPD) molecules. In the present study, we focus on the properties of individual nanoparticles by measuring the adhesion force between the AFM tips and the particle surface. The results further confirm the amphiphilic nature of the Janus particles.

Experimental Procedures

Chemicals. Hydrogen tetrachloroauric acid ($HAuCl_4$) was synthesized by dissolving ultrahigh purity gold (99.999%, Johnson Matthey) in freshly prepared aqua regia followed by crystallization.[27] Tetraoctylammonium bromide (Alfa Aesar, 98%), hexanethiol (C6SH, Acros, 96%), sodium borohydride ($NaBH_4$, Acros, 99%), tetrahydrofuran (THF, Acros, 99.5%), ethanol (Fischer, 100%), and 3-mercaptopropane-1,2-diol (MPD, Aldrich, 95%) were all used as received. Solvents were purchased from typical commercial sources at their highest purities and used without further treatments. Water was supplied by a Barnstead Nanopure water system (18.3 MΩ).

Particle Synthesis. The hexanethiolate-protected gold (AuC6) nanoparticles were synthesized by using the Brust et al. protocol.[28] The particles then underwent careful fractionation by using a binary solvent−nonsolvent mixture of toluene and ethanol. The fraction with the smallest average core diameter was used in the subsequent studies.

The detailed procedure to prepare Janus nanoparticles has been reported earlier,[26] where the AuC6 particles were used as the starting particles and MPD as the hydrophilic ligands. In a typical experiment, 300 µL of the AuC6 particle solution at a concentration of 1 mg/mL in toluene was spread in a dropwise fashion onto the water surface of a Langmuir−Blodgett trough (NIMA Technology, Model 611D) with a Hamilton microliter syringe.[29] At least 1 h was allowed for solvent evaporation and between compression cycles. The barrier speed was controlled at 10 cm²/min. The particle monolayer was compressed to a desired surface pressure where the interparticle edge-to-edge separation was maintained at a value somewhat smaller than twice the extended ligand chain length. This resulted in ligand intercalation between adjacent particles and hence impeded the interfacial mobility of the particles. At this point, a calculated amount of MPD ligands was injected into the water subphase by a Hamilton microliter syringe. The particles were kept at the same surface pressure for an extended period of time (typically 8 h) before the particles were collected by a Pasteur pipet. Excessive free MPD ligands were removed by solvent extraction, where the particles were dissolved in dichloromethane and the MPD ligands in water. ¹H NMR measurements indicated that approximately 50% of the original hexanethiolate ligands was replaced by the hydrophilic MPD molecules.[26]

Preparation of AFM Samples. Thin films of Au(111) on mica were purchased from Molecular Imaging Inc. and used as the substrates. Prior to use, the gold surfaces (1.0 cm × 1.1 cm) were cleaned in UV-ozone for 10 min (Model 42, Jelight Co.). The gold films were then immersed into a 1 mM solution of C6SH or MPD in ethanol for 24 h for the formation of a self-assembled monolayer (SAM) with either hydrophobic (C6 SAM) or hydrophilic (MPD SAM) characteristics. The substrates were rinsed with excessive ethanol and blow-dried in a gentle stream of nitrogen before the

(27) Brauer, G. *Handbook of Preparative Inorganic Chemistry*, 2nd ed.; Academic Press: New York, 1963.

(28) Brust, M.; Walker, M.; Bethell, D.; Schiffrin, D. J.; Whyman, R. *J. Chem. Soc., Ser. Chem. Commun.* **1994**, 801−802.

(29) Chen, S. W. *Langmuir* **2001**, *17*, 6664−6668.

Scheme 1. Schematic Representations of Interaction between Unmodified Tip and (a) C6 SAM-Modified Au(111), (b) Janus Particles on C6 SAM-Modified Au(111), (c) AuC6 Particles on C6 SAM-Modified Au(111), (d) MPD SAM-Modified Au(111), and (e) Janus Particles on MPD SAM-Modified Au(111)
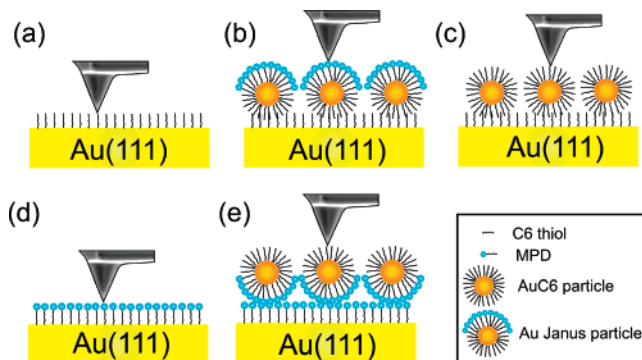
deposition of nanoparticles. To prepare the particle samples for AFM measurements, a calculated amount (∼20 µL) of a dilute THF solution (of the order of micromolar amounts) containing the original AuC6 nanoparticles or Janus nanoparticles was dropcast onto the C6 SAM or MPD SAM-modified Au(111) substrate surface. The evaporation of the volatile solvent at ambient temperature resulted in the immobilization of the particles on the substrate surfaces with the orientation of the particles determined by the surface wettability.

AFM Measurements. AFM images were acquired under ambient conditions with a PicoLE SPM instrument (Molecular Imaging) in the tapping mode. The tapping mode cantilevers exhibited resonant frequencies between 120 and 190 kHz (typically 165 kHz), force constants of 2.5−8.5 N/m, and tip apex radii of ∼10 nm. The resulting images were flattened and plane-fitted using software from Molecular Imaging. Because of tip convolution, particles appeared larger in diameter, and the particle size was estimated by the heights in the AFM images (note that the height reflects the summation of the particle core plus two ligand lengths). The force−distance curves were obtained in the contact mode. Contact mode cantilevers are ultrasharp silicon tips with resonant frequencies between 8.5 and 15 kHz, force constants of 0.05 to ∼0.30 N/m (typically 0.15 N/m), and tip curvature radii smaller than 10 nm. Before force measurements, large areas (∼1500 nm²) were scanned first to obtain a stable image without obvious drift. Individual particles with diameters in the range of 5−15 nm were selected for the adhesion force measurements. For nanoparticles smaller than 5 nm, the tip−gold surface interaction became the dominating component of the adhesion force. Particles larger than 15 nm were not selected to minimize the possible complication of particle aggregates.

Results and Discussion

C6 SAM-Modified Au(111). The AFM cantilever and probe system was used as an ultrasensitive force apparatus to detect the interactions between the tip and the sample surface. We first used the AFM cantilever tip and the C6 SAM coated substrate to measure the forces as they were brought into and out of contact (Scheme 1a). The maximum cantilever deflection during the retraction phase is related to the magnitude of the force required to break the interactions between the tip and the substrate. Figure 1a depicts a representative force−distance curve of the interactions between the AFM tip and the C6 SAM-coated Au(111) substrate. It can be seen that the adhesion force was about 26 nN. Ten sets of measurements (each consisting of 50 force measurements) were taken at different substrate locations. The collective histogram of the adhesion force is presented in Figure 1b. The distribution is quite narrow, and the mean value of the adhesive force is 26.0 ± 9.5 nN, which is somewhat higher than that
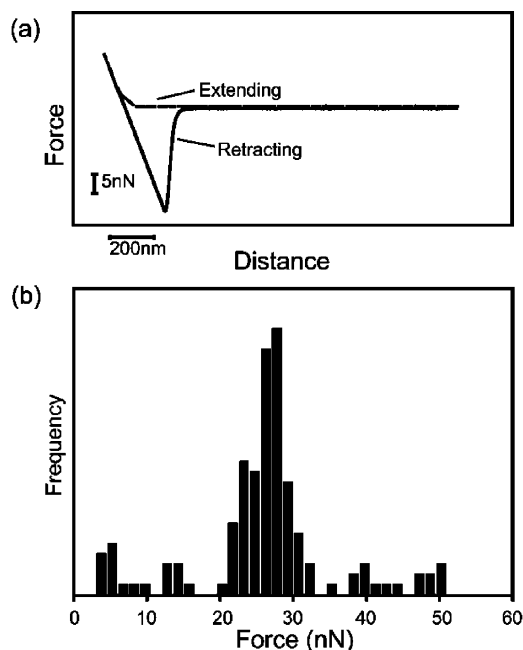
Figure 1. (a) Representative force−distance curve and (b) histogram of the adhesion force between the tip and the C6 SAM-modified Au(111) surface.

measured for similar methyl-terminated thin films in air but with a Si_3N_4 tip (ca. 12 nN).[30,31] It should be noted that the AFM cantilever spring constant was not quantitatively calibrated here and that the typical spring constants provided by the manufacturer were used in our calculations. Therefore, a systematic error may be included in the value of the calculated force. Additionally, this adhesion force may also include the contribution from the interactions between the tip and a possible water layer on the sample surface. Since the experiments were carried out in ambient humidity, it is likely that water formed a capillary bridge between the tip and the sample.[32,33]

On the basis of the previous study, we assembled the Janus particles onto the C6 SAM/Au(111) surface by dropcasting a very dilute THF solution of the Janus nanoparticles (Scheme 1b). A typical AFM image in the tapping mode is shown in Figure 2a, where individual Au Janus particles within a size range of 2−9 nm can be seen. A detailed size distribution of the Janus particles is shown in the inset to Figure 2a. In addition to the features of nanoparticles, some cracks and holes can also be observed from the AFM image, which are ascribed to the defects of the Au substrate, as evidenced by tapping mode AFM measurements of the naked Au substrates. The force−distance curves were then recorded in the contact mode to examine the interactions between AFM probes and individual Janus particles. A typical force−distance curve is shown in Figure 2b, where the adhesion force is about 32 nN. Ten sets of measurements (each consisting of 20 force measurements) were acquired at different particles. The histogram of the adhesion forces is presented in Figure 2c, and the mean value of the adhesion force is found to be 31.5 ± 10.0 nN.

For comparison, we repeated the measurements but used the original AuC6 nanoparticles instead of the Janus particles (Scheme
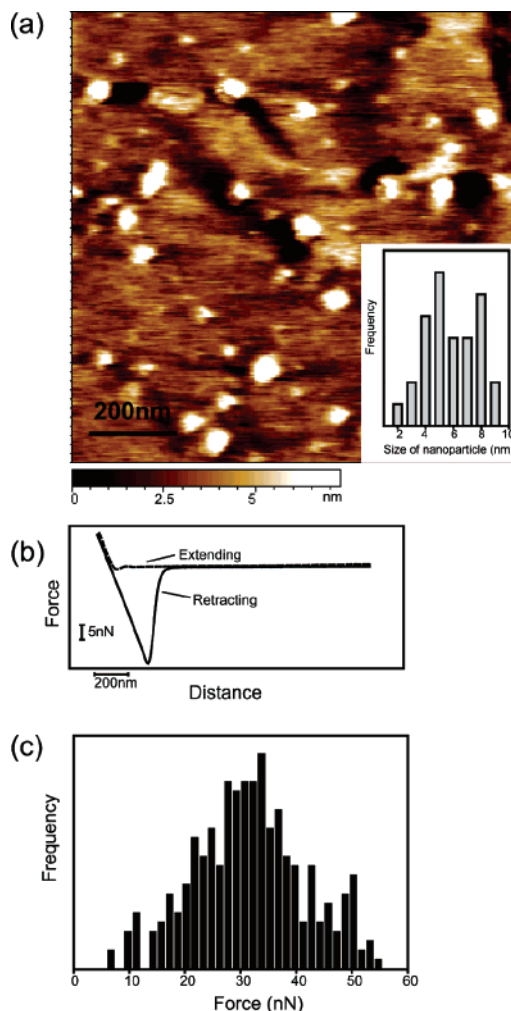
(30) Subramanian, S.; Sampath, S. *Pramana* **2005**, *65*, 753−761.
(31) Noel, O.; Brogly, M.; Castelein, G.; Schultz, J. *Langmuir* **2004**, *20*, 2707−2712.
(32) Piner, R. D.; Zhu, J.; Xu, F.; Hong, S. H.; Mirkin, C. A. *Science* **1999**, *283*, 661−663.
(33) Garno, J. C.; Yang, Y. Y.; Amro, N. A.; Cruchon-Dupeyrat, S.; Chen, S. W.; Liu, G. Y. *Nano Lett.* **2003**, *3*, 389−395.

Figure 2. (a) Representative AFM image of Janus particles on the C6 SAM-modified Au(111) surface acquired in tapping mode, scan rate 2.3 lines/s. Inset shows the size distribution of the Janus particles. (b) Typical force−distance curve and (c) histogram of the adhesion force between the tip and the Janus particles on C6 SAM-modified Au(111).

1c). The topographic AFM image in the tapping mode is shown in Figure 3a. Individual AuC6 particles can be seen clearly on the C6 SAM/Au(111) surface. According to the size distribution (shown as the inset in Figure 3a), the AuC6 particles are in the range of 2−15 nm. A total of 200 force−distance measurements between the tip and the AuC6 particles were then carried out at different particles. A typical force−distance curve and the histogram of the adhesion force are shown in Figure 3b,c, respectively. The mean force between the tip and the AuC6 particles is 27.5 ± 4.5 nN. This is very close to the mean force estimated above for the direct contact between the AFM tip and the C6 SAM surface (Figure 1) but somewhat lower than that between the tip and the Janus nanoparticles (Figure 2). The former may be interpreted by the similarity in terms of the chemical functionality of the substrate surface, both of which involve methyl terminal groups, whereas the large discrepancy as compared to the result of the Janus nanoparticles may be ascribed to the oriented assembly of the Janus nanoparticles on the C6 SAM/Au(111) surface (Scheme 1b), where most likely the particles adopted a conformation with the hydrophobic side in direct contact with the C6 SAM surface, whereas the hydrophilic side was exposed. Thus, the stronger interactions between the hydrophilic (silicon) AFM tip and the hydrophilic side of the Janus particles are reflected by a greater adhesion force.
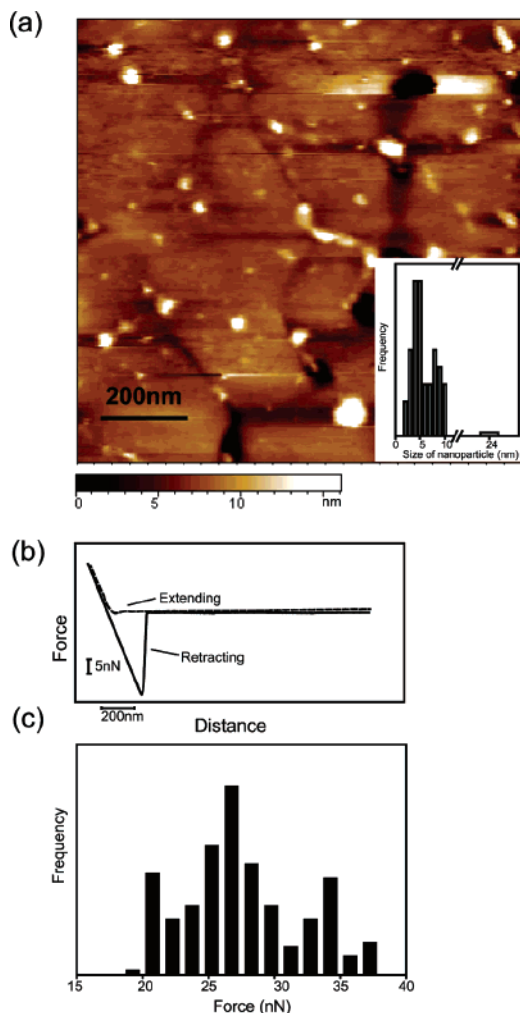
Figure 3. (a) Representative AFM image of AuC6 particles on the C6 SAM-modified Au(111) surface acquired in tapping mode, scan rate 2.3 lines/s. Inset shows the size distribution of the AuC6 particles. (b) Typical force−distance curve and (c) histogram of the adhesion force between the tip and the AuC6 particles on the C6 SAM-modified Au(111).

The above observations are consistent with previous investigations of the adhesion force between hydrophilic/hydrophobic tips and hydrophilic/hydrophobic substrate surfaces. For instance, Lieber and co-workers[34,35] chemically modified an AFM tip and examined the force versus distance curves recorded under EtOH. Their results showed that the tip−substrate interactions varied drastically with their respective chemical functionalities, which decreased in the order of COOH/COOH > CH_3/CH_3 > COOH/CH_3. Although the absolute values of the adhesion force are different from our data due to the different experimental conditions, the changing trend remains the same, that is, the interactions between a hydrophilic tip and a hydrophilic substrate are greater than those between a hydrophilic tip and a hydrophobic substrate.

MPD SAM-Modified Au(111). Consistent results were also obtained by using the MPD-modified Au(111) substrate. First, the interactions between the AFM tip and the MPD-modified Au(111) were investigated in contact mode (Scheme 1d). Again, a representative force−distance curve is shown in Figure 4a, with an adhesion force of about 34 nN. From the force histogram
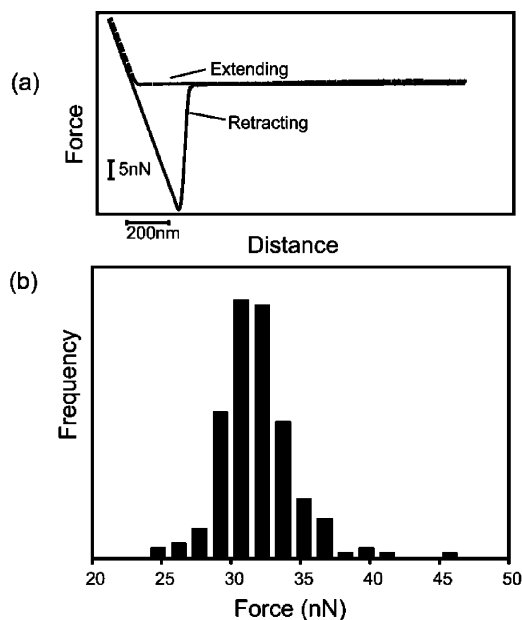
(34) Noy, A.; Frisbie, C. D.; Rozsnyai, L. F.; Wrighton, M. S.; Lieber, C. M. *J. Am. Chem. Soc.* **1995**, *117*, 7943−7951.

(35) Noy, A.; Vezenov, D. V.; Lieber, C. M. *Ann. Rev. Mater. Sci.* **1997**, *27*, 381−421.
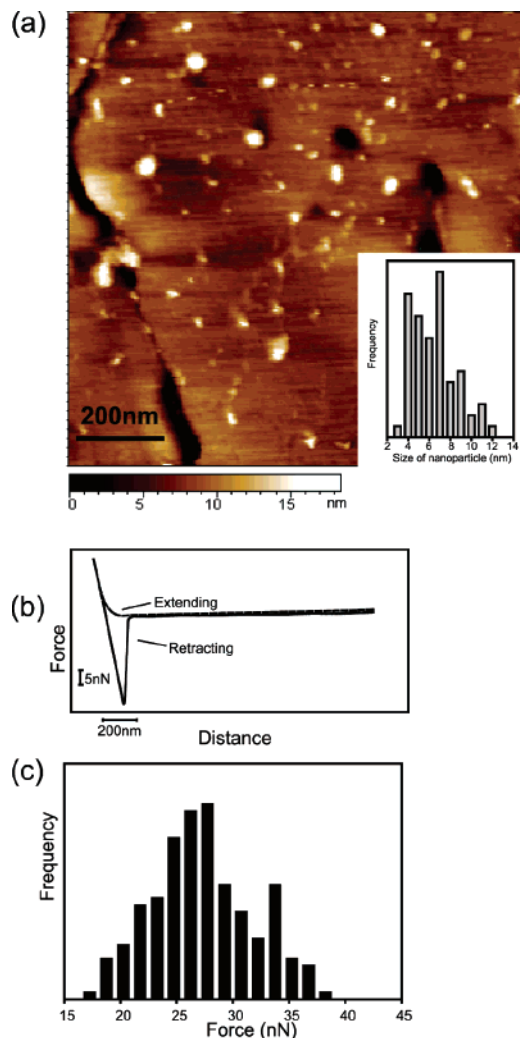

Figure 4. (a) Representative force−distance curve and (b) histogram of the adhesion force between the tip and the MPD SAM-modified Au(111).

(Figure 4b) based on 200 measurements at different sites, the mean force between tip and MPD-modified Au(111) is 31.9 ± 2.7 nN. This is somewhat greater than that observed above for the C6 SAM-modified Au(111) surface (and the AuC6 particles on the same substrate surface), again, because of the enhanced interactions between the hydrophilic MPD surface and the silicon AFM tip. Yet, it is close to the mean force with the Janus particles immobilized onto the C6 SAM/Au(111) surface, consistent with the oriented assembly of the Janus nanoparticles on the surface.

In the subsequent study, the Janus particles were deposited onto the MPD SAM/Au(111) surface by, again, dropcasting a dilute THF solution of the particles (Scheme 1e). A typical tapping mode AFM image of the Janus particles on the MPD SAM/Au(111) surface is shown in Figure 5a. The individual particles within a size range of 2−12 nm can be seen (Figure 5a, inset). Then, contact mode AFM was again employed to investigate the interactions between the tip and the Janus particles. A representative force−distance curve is shown in Figure 5b, which reveals an adhesion force of about 30 nN. Similarly, 200 force curves were collected at 10 different sites. The force histogram is shown in Figure 5c, where the mean force is estimated to be 27.3 ± 4.5 nN. This is very similar to the mean forces measured with the C6 SAM/Au(111) surface and with the AuC6 particles immobilized onto the C6 SAM/Au(111) surface, again suggesting oriented arrangements of the Janus particles on the MPD SAM-modified surface with the hydrophobic side exposed.

Table 1 summarizes the adhesion forces measured in these different systems. It should be noted that the adhesion force in air consists of two parameters. One is the force associated with the sample's structure and surface energy, the other one is the capillary force at the interface. In principle, the capillary force depends on the surface tension of the sample, the tip, as well as on the tip radius and air humidity. In our study, the tip is unfunctionalized silicon and thus is assumed to possess a native oxide layer (which is hydrophilic). Note that before every measurement, the tip was cleaned in UV-ozone for 1 h; thus, the possibility of the presence of organic contaminants on the tip surface was minimized. The air humidity was also kept constant. Thus, the similar adhesion force observed in systems 1, 3, and 5 (Table 1) is likely ascribed to the fact that all the surfaces

Table 1. Summary of Mean Adhesion Forces between AFM Tips and Varied Surface Thin Films

no.	substrate	particle	mean force (nN)
1	C6 SAM-modified Au(111)	no particle	26.0 ± 9.5
2		Au Janus particles	31.5 ± 10.0
3		AuC6 particles	27.5 ± 4.5
4	MPD SAM-modified Au(111)	no particle	31.9 ± 2.7
5		Au Janus particles	27.3 ± 4.5

and the SAM/Au(111) surface will most likely vary with the size of the particles. Nevertheless, it should be noted that the size range of the particles under study is statistically identical, based on the particle size histograms. Thus, the effect on the force distribution is anticipated to be comparable. Second, the orientation of the Janus nanoparticles may deviate from the ideal situation that is depicted in Scheme 1. In fact, one can see that the adhesion force for the AuC6/C6 SAM-Au(111) system was mostly confined within the range of 20−35 nN (Figure 3), whereas for the Janus particles/C6 SAM-Au(111), the force was found in a much wider range of 10−55 nN (Figure 2) and for Janus/MPD SAM-Au(111), 15−40 nN (Figure 5). This discrepancy can be, at least partly, attributable to the orientational variation of the Janus nanoparticles, as compared to the isotropic nature of the AuC6 surface.

Conclusion

In this study, the amphiphilic nature of the Janus nanoparticles was examined by measuring the adhesion force between the AFM tip and the particle surface. When the Janus nanoparticles were dropcast onto a substrate surface, the particles adopted a conformation that maximized the interactions with the substrate surface. The hydrophobic (hydrophilic) hemisphere of the Janus particles was exposed when a hydrophilic (hydrophobic) substrate surface was used, resulting in a substantial discrepancy in the adhesion force measurements between the AFM tip and the particles. Although a systematic error may be included in the absolute values of the adhesion force due to the meniscus forces exerted by thin layers of water vapor and uncalibrated spring constants of the cantilevers, the results presented herein provide further confirmation of the amphiphilic characters of the Janus nanoparticles.

In ongoing work, we intend to study the tip−sample interactions in a controlled atmosphere or in a liquid environment, which will eliminate the influence of capillary water on the adhesion interactions.

Figure 5. (a) Representative AFM image of Au Janus particles on MPD SAM-modified Au(111) acquired in tapping mode, scan rate 2.3 lines/s. Inset shows the size distribution of the Janus particles. (b) Typical force−distance curve and (c) histogram of the adhesion force between the tip and the Janus particles on MPD SAM-modified Au(111).

exhibit the same methyl −(-CH$_3$) termination, which results in similar surface energies and hence similar pull-off forces, whereas results of systems 2 and 4 can be explained on the basis of their similar OH-terminated surfaces (Scheme 1). All these measurements suggest an oriented assembly of the Janus nanoparticles as manipulated by the substrate hydrophobicity.

Finally, while overall the force histograms all exhibit a rather narrow distribution, the slight variation of the adhesion force within each group of measurements may arise from at least two sources. The first is related to the dispersity of the particle dimensions. As the tip radius is larger than the nanoparticles under study, contributions from the interactions between the tip